2007-02-01

Application of Advanced Computational Modelling in the Comparison of Stent Induced Coronary Flow Disturbances

Jonathan Murphy
Technological University Dublin, jonathan.murphy@tudublin.ie

Fergal Boyle
Technological University Dublin, fergal.boyle@tudublin.ie

Recommended Citation

Murphy, J., Boyle, F.: Application of Advanced Computational Modelling in the Comparison of Stent Induced Coronary Flow Disturbances. The Fifth IASTED International Conference of Biomedical Engineering, 2007.

Funder: Department of Mechanical Engineering, Technological University Dublin (DIT)and the Irish Research Council for Science Engineering and Technology (IRCSET) under the Embark Initiative part of the National Development Plan

APPLICATION OF ADVANCED COMPUTATIONAL MODELLING IN THE COMPARISON OF STENT INDUCED CORONARY FLOW DISTURBANCES

Jonathan Murphy, Fergal Boyle
Department of Mechanical Engineering
Dublin Institute of Technology
Bolton Street, Dublin 1
Ireland
jonathan.murphy1@student.dit.ie

ABSTRACT
Coronary stent implantation can improve blood flow in an artery narrowed by the build up of arterial plaque. However, the haemodynamic effect of stent placement is unclear and may influence arterial restenosis (re-blockage). In this investigation computational fluid dynamics (CFD) was used to predict the non-Newtonian three-dimensional flow field in a coronary artery following implantation of two different stents. A graphical illustration of the stented areas affected to various degrees of wall shear stress (WSS) is presented for both the Palmaz-Schatz (PS) and the Gianturco-Roubin-II (GR-II) coronary stents. The axial WSS and wall shear stress gradient (WSSG) is also presented graphically over one stent strut for each stent. Finally, a comparison is drawn between the CFD results and restenosis data from a clinical trial.

KEY WORDS
Computational fluid dynamics, wall shear stress, and stents

1. Introduction

Coronary artery disease (CAD) is one of the leading causes of death in the developed world. CAD occurs due to the build up of plaque in the coronary arteries which supply fresh blood to the constantly active heart muscle. This build up of plaque, a condition known as atherosclerosis, deprives the heart muscle of its crucial supply of oxygen and nutrients provided by the coronary blood supply. In the past a coronary artery bypass graft was the only treatment available for CAD. This is a large scale operation involving the sawing open of the breastbone and grafting of a blood vessel to bypass the site of the blockage.

Percutaneous transluminal coronary angioplasty (PTCA) was introduced in the late 1970s as a minimally invasive procedure to relieve the narrowing in a coronary artery due to the build up of plaque. PTCA is accomplished with a small balloon catheter inserted into an artery in the groin or arm, and advanced to the narrowing in the coronary artery. The balloon is then inflated to enlarge the narrowing in the artery and restore blood flow to the heart muscle. However in over 40% of patients treated with PTCA the artery becomes re-blocked within six months in a process known as restenosis [1]. This is largely due to elastic recoil of the vessel wall [2].

In the early 1990s stents were introduced to improve the success rates of PTCA. Basically, a stent is an expandable, slotted metal tube inserted into the artery. It acts as a scaffold to provide support for the artery and has proven effective at eliminating elastic recoil, one mechanism of restenosis that can result in re-blockage [2]. The use of stents has shown more promising clinical outcomes than PTCA alone. However, restenosis remains a persistent problem with restenosis rates generally as high as 20% at six months after intervention [3].

The changes in WSS induced by an implanted stent play a significant role in the immunological behaviour of the coronary artery. This behaviour is directly linked to restenosis within the stented artery [4, 5]. In order to assess the haemodynamic impact of coronary stent implantation, three-dimensional computational models of a stented left anterior descending (LAD) coronary artery have been created using computer-aided-design. One model represents the artery implanted with a PS stent and the second model represents the artery implanted with a GR-II stent. CFD was used to simulate the flow field of the coronary artery with the implanted stent in each case.

Results are shown of the mesh convergence studies conducted. Contour plots and graphs of areas of high and low WSS and a graph of the axial WSSG in the vicinity of struts for both stents are also presented. The GR-II stent has been shown to perform poorly against the PS stent in a recent medical trial. The CFD results presented suggest that this poor performance is a direct result of the stent induced haemodynamic factors.

2. Stents

2.1 Introduction

Stents are small tubular prostheses that serve the purpose of maintaining an adequate inner diameter of a narrowed blood vessel to allow for the comfortable passage of the blood. In 1986 Jacques Puel and Ulrich Sigwart implanted the first coronary wallstents in Toulouse, France. Today over 1 million stents are implanted worldwide each year. A stent is

mounted on a balloon-tipped catheter, threaded through the artery, and positioned at the site of the blockage. As shown in Figure 1 the balloon is then inflated, opening the stent. Subsequently, the catheter and deflated balloon are removed, leaving the stent lodged in place against the inner lining of the artery.

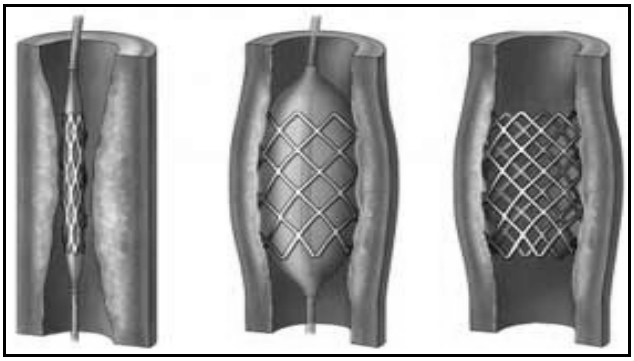

Figure 1: The stenting procedure for a narrowed artery.

2.2 Stent Design

The two stent designs modelled using CFD are shown in Figures 2 and 3 below. The first is the PS coronary stent manufactured by Johnson and Johnson. The stent is 15 mm long, consisting of two 7 mm sections joined by a 1 mm bridge. It ranges from 3 mm to 4 mm in diameter and is a slotted tube balloon expandable design. The second type of stent is the GR-II which is manufactured by Cook. The GR-II stent has a balloon expandable coil design and is produced in 20 mm and 40 mm lengths ranging from 2.5 mm to 4 mm in diameter.

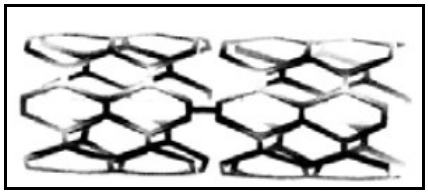

Figure 2: The Palmaz-Schatz coronary stent developed by Johnson and Johnson.

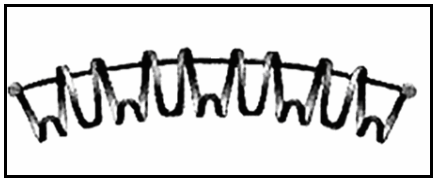

Figure 3: The Gianturco-Roubin II coronary stent developed by Cook.

2.3 Mechanism of Stent Restenosis

The implantation of a coronary stent leads to vascular injury and haemodynamic effects which may result in restenosis. Under normal healthy conditions vascular smooth muscle cells (VSMC) reside in the lunica media which is shown in the arterial cross section in Figure 4. Stent restenosis occurs when VSMC migrate through the lunica intima which is the inner lining of the artery wall, and build up in the artery lumen restricting the blood flow, a process known as neointimal hyperplasia (NH). The main components that determine the degree of restenosis that will occur are the blood clotting platelets which flow through the artery lumen and the endothelial cells (EC) which form the lunica intima.

Platelets flowing in the artery lumen will bind together to form a blood clot if they become activated. Platelets can be activated through contact with a number of different substances such as thrombin or platelet derived growth factor (PDGF). Activated platelets will themselves release these substances to activate platelets around them. However, PDGF also has the effect of triggering NH. It has been documented that the platelet deposition near the stent in the first twelve hours after stenting is a major indicator of the amount of NH that will occur [6].

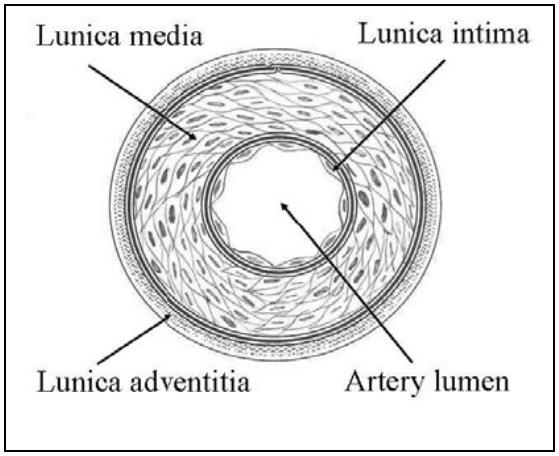

Figure 4: Cross section of a coronary artery.

Platelets and endothelial cells are directly affected by the shear force exerted by the flowing blood on the artery lumen wall known as WSS. It has been shown in a two-dimensional CFD study that areas of low velocity flow and low WSS exist in the vicinity of newly implanted stent wires [7]. The platelet deposition and residence times are much higher in these stagnation areas. This leads to platelet accumulation in the area around the stent wire leading to increased NH formation. The stent induced changes in the haemodynamics of the coronary flow also lead to an alteration of the WSS exerted on the EC [5, 8]. WSS has been shown to have a significant effect on the behaviour of EC [9]. A healthy value for WSS in a coronary artery is approximately 1.5 Pascals [10]. When EC are subjected to values of WSS lower than this they begin to release adenosine diphosphate and triphosphate which induces platelet activation leading to blood clotting and NH formation [9]. Conversely, when endothelial cells are subjected to areas of "healthy" WSS they secrete nitrous oxide (NO) which inhibits adhesion of platelets to the vessel wall and VSMC growth, hence inhibiting NH formation [10]. Numerous studies have shown a link between areas of low WSS and increased NH [4, 5].

The success of a stenting procedure relies heavily on the reendothelialisation of the vessel wall after implantation and the successful function of the newly formed endothelial cells to inhibit platelet deposition. If a new layer of EC successfully grows over the stent the NH formation will cease. In a study to demonstrate the effect of wall shear stress gradients (WSSG), EC were exposed to a region of

separated flow. After 48 hours the major finding was that in the area of the highest WSSG the EC density was up to 40% less than experimental controls [11]. Through the inhibition of reendothelialisation, high WSSG contribute to NH formation [5].
EC will be damaged by the stenting procedure leading to the release of platelet activating substances and NH formation. A relationship has been established between vascular injury and NH [12].
Areas of low WSS, areas of high WSSG, and vascular injury at the time of stent implantation are the main contributors to NH formation. In light of this, disturbances to the coronary blood flow and the degree of trauma to the vessel wall due to stent implantation cannot be overlooked in future stent design.

3. CFD Analysis

3.1 Introduction

CFD is a process whereby real-life fluid flows are simulated using numerical methods to solve the governing equations of fluid dynamics. CFD is a relatively new branch of fluid dynamics commonly regarded as the "third" technique for solution of fluid flow problems, complementing, but not replacing the well-established approaches of theory and experiment. CFD finds it niche in modelling fluid flows that are difficult or impossible to model using theory and are complex, time consuming or expensive to measure experimentally.

3.2 The Computational Model

In both computational models a cylindrical domain was created and the stent design cut from the domain to simulate conditions of the stent semi-embedded in the artery wall. One of the 7 mm sections of the PS stent was modelled and a half section of the 20 mm long GR-II stent was modelled.
The domain extended 2.5 mm proximal (upstream) and 2.5 mm distal (downstream) of the stent in each case to capture the flow field in those regions.

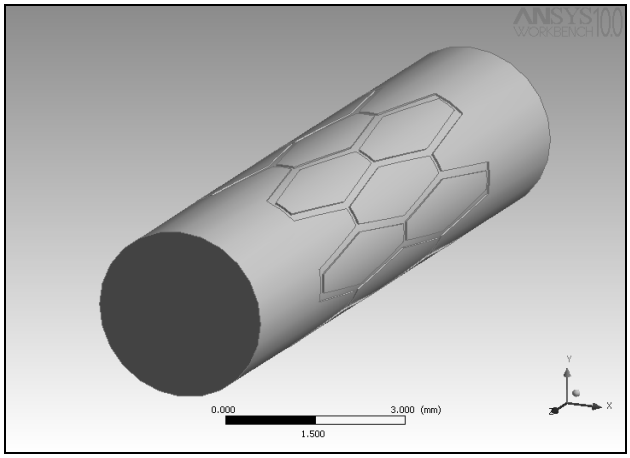

Figure 5: Computational domain representing the left anterior descending coronary artery with implanted PS stent.

3.3 Governing Equations of Fluid Mechanics

Both simulations involved steady laminar flow which requires the CFD code to solve the conservation of mass and momentum equations, of which the general form are listed as Equations (1) and (2) respectively:

$$\frac{\partial \rho}{\partial t} + \nabla.\left(\rho \vec{V}\right) = 0 \tag{1}$$

$$\frac{\partial \rho \vec{V}}{\partial t} + \nabla.\left(\rho \vec{V} \otimes \vec{V}\right) = -\vec{\nabla} p + \vec{\nabla}.(\tau) + \rho \vec{g} + \vec{F} \tag{2}$$

where ρ is the fluid density, p is the static pressure, $\vec{V}$ is the velocity vector, $\vec{F}$ represents external body forces such as gravity, μ is the fluid dynamic viscosity and τ is the shear stress tensor given by Equation (3):

$$\tau = \mu\left(\nabla \vec{V} + \nabla \vec{V}^{T}\right) \tag{3}$$

At low shear rates blood exhibits the non-Newtonian behaviour of variable dynamic viscosity which is dependant on the shear rate. The non-Newtonian nature of the flow is accommodated by using the Carreau model [13] given in Equation (4):

$$\mu = \mu_{\infty} + (\mu_0 - \mu_{\infty})\left[1 + (\gamma\lambda)^2\right]^{\left(\frac{q-1}{2}\right)} \tag{4}$$

where γ is the rate of deformation tensor given by Equation (5) for a three-dimensional Cartesian coordinate system

$$\gamma = \left[\begin{array}{l} 2\left\{\left(\frac{\partial v_x}{\partial x}\right)^2 + \left(\frac{\partial v_y}{\partial y}\right)^2 + \left(\frac{\partial v_z}{\partial z}\right)^2\right\} \\ + \left(\frac{\partial v_x}{\partial y} + \frac{\partial v_y}{\partial x}\right)^2 + \left(\frac{\partial v_x}{\partial z} + \frac{\partial v_z}{\partial x}\right)^2 + \left(\frac{\partial v_y}{\partial z} + \frac{\partial v_z}{\partial y}\right)^2 \end{array} \right]^{\frac{1}{2}} \tag{5}$$

and the constants for the Carreau model given below have been established from experimental data [13]:

$$\begin{array}{ll} \mu_0 = 0.056 \text{ Pa.s} & \lambda = 3.31 \text{ s} \\ \mu_{\infty} = 0.00345 \text{ Pa.s} & q = 0.375 \end{array} \tag{6}$$

The highly sophisticated commercial software code CFX™ was used to solve the governing equations of fluid mechanics for non-Newtonian blood flow in the computational domain using a vertex-centred finite volume scheme.

3.4 Boundary Conditions

The same boundary conditions were applied at the inlet, outlet and on the walls for both simulations.

3.4.1 Inlet Boundary

A fully developed axial velocity profile was applied at the inlets given by:

$$V = V_{Max}\left(1-\frac{r^2}{R^2}\right) \qquad (7)$$

where the variable r is the radius measured from the centreline at any point on the inlet plane and R is the radius at the wall of the domain. V_{Max} is the maximum centreline velocity given a value of 0.412 m/s in Equation (7) to simulate resting conditions in the LAD coronary artery [14].

3.4.2 Outlet Boundary

A static pressure of zero Pascals was applied at the outlets of the both domains, allowing the software to calculate the velocity at these planes.

3.4.3 Wall Boundary

The no-slip boundary condition was applied on all surfaces representative of the artery wall and the stent wires.

3.5 Computational Mesh

Analytical solutions to the governing equations of fluid mechanics exist for only the simplest of flows under ideal conditions. To obtain solutions for real flows a numerical approach must be adopted whereby the equations are replaced by algebraic approximations which may be solved using a numerical method. To achieve this, the computational domain must be divided into a set of much smaller non-overlapping sub-domains called elements which constitute the mesh. To obtain an accurate solution a sufficient number of elements must be placed in the computational domain. Figure 6 shows the fine mesh employed in the area around the PS stent wires.

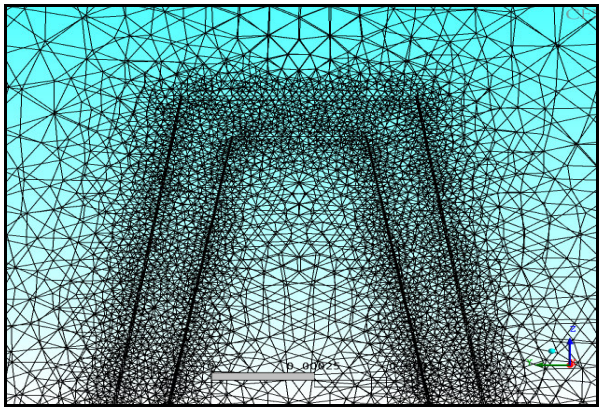

Figure 6: Computational mesh in the vicinity of a PS stent strut.

4. Results

4.1 Mesh Convergence Study

A mesh convergence study was carried out to establish the required mesh density for accurate solutions, such that any increase in nodes would lead to no appreciable difference in the solution. Mesh convergence was achieved for both simulations by sequentially increasing the number of nodes until there was no appreciable difference in the axial distribution of WSS across one of the stent struts between the solutions.

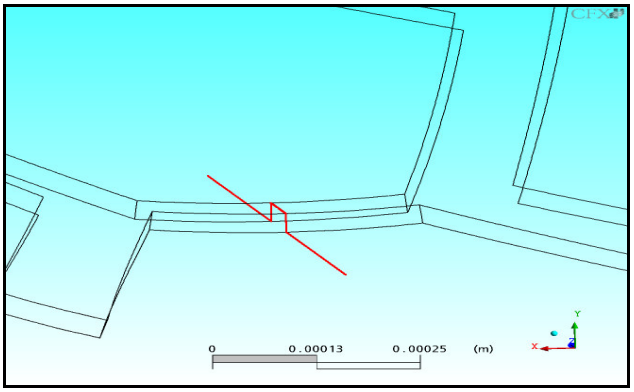

Figure 7: PS Stent strut and sample line upon which mesh convergence study was carried out.

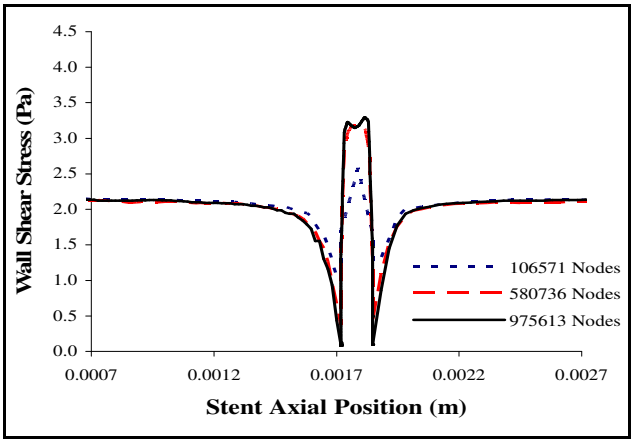

Figure 8: Axial distributions of WSS across a PS stent strut as calculated by successively refined computational meshes.

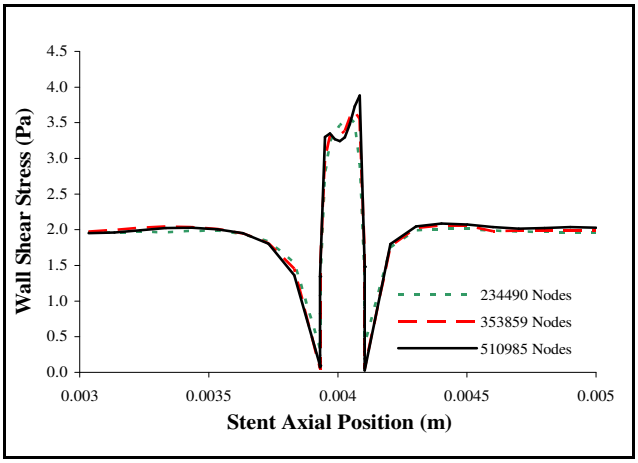

Figure 9: Axial distributions of WSS across a GR-II stent strut as calculated by successively refined computational meshes.

4.2 Wall Shear Stress Results

The predicted three-dimensional flow field reveals areas of high WSS on the tops of the stent struts and low WSS

immediately proximal and distal to the stent struts, particularly those transversal to the blood flow as shown in Figures 10 and 11. Figure 12 illustrates the percentage stented area subjected to WSS below a given magnitude starting from 0.1 Pascals. In comparison to the PS stent, the GR-II stent has more than double the percentage stented area subjected to WSS less than 0.1 and 0.25 Pascals, and 70% more percentage stented area subjected to less than 0.5 Pascals. The GR-II stent also has areas on the stent wires with higher WSS than the PS stent with a maximum WSS value of 4.28 Pascals compared to the PS stent which has a maximum of 3.73 Pascals.

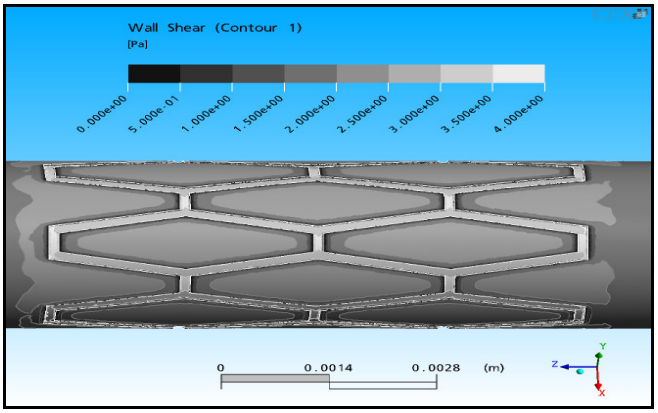

Figure 10: Contour map of WSS in the vicinity of the implanted PS coronary stent.

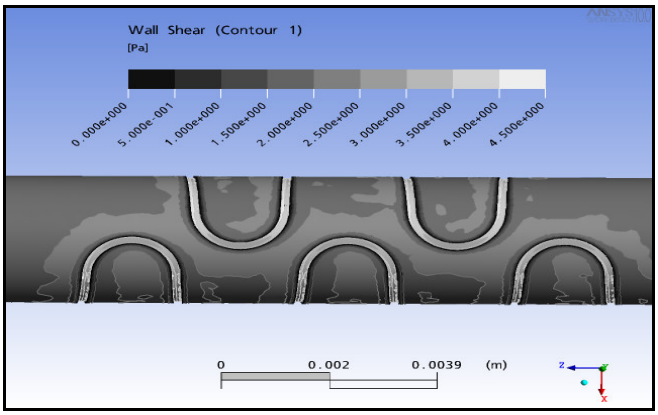

Figure 11: Contour map of WSS in the vicinity of implanted GR-II coronary stent.

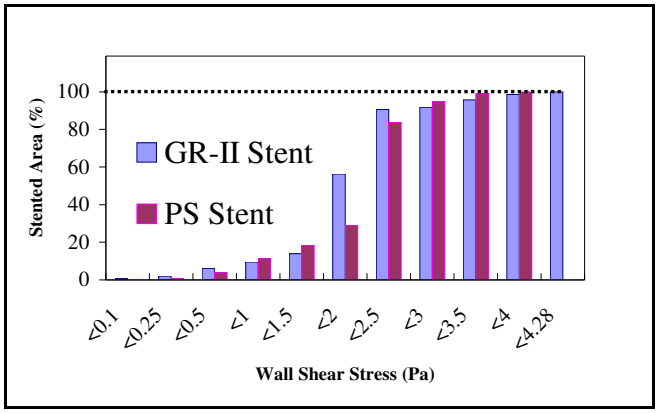

Figure 12: Bar chart illustrating percentage stented area subjected to varying degrees of WSS for the GR-II and PS stent

Figures 13 and 14 show the axial distribution of WSS and WSSG over one stent strut transversal to the flow direction which is where the maximum WSSG appears as shown in Figures 10 and 11. The magnitude of low WSS on both sides of the strut is similar for both stents. However, the GR-II stent displays 15% higher WSS on the top of the stent strut than the PS stent leading to a 21% higher WSSG in front of the stent strut and a 44% increase in WSSG behind the strut.

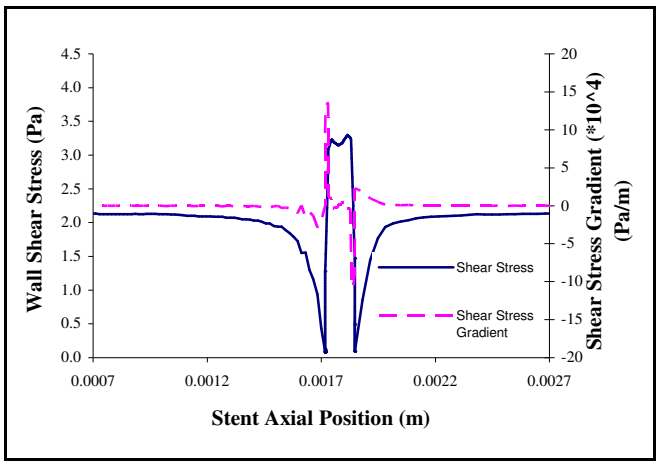

Figure 13: Distribution of WSS and WSSG in the axial direction over one of the PS stent struts.

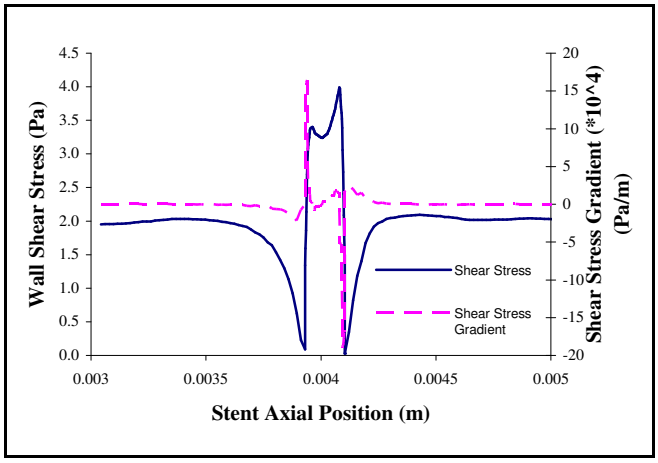

Figure 14: Distribution of WSS and WSSG in the axial direction over one of the GR-II stent struts.

5. Conclusion

It is clear that haemodynamics of the flow in an artery implanted with a stent have an effect on the immunological response within the vessel wall of that artery. This work has demonstrated that stent design has an effect on those haemodynamic characteristics.

In a medical trial conducted to compare the in vivo performance of these two stents, the GR-II stent had a restenosis rate of 47.3% compared to the PS restenosis rate of 20.6% after six months [15]. Areas of low WSS and high WSSG have earlier been identified as factors which encourage the development of NH which leads to restenosis. The CFD results predict that implantation of the GR-II stent

rather than the PS stent would produce 70% more percentage stented area subjected to WSS below a value of 0.5 Pa. Implantation of a GR-II stent would also lead to up to 44% more WSSG around the stent struts. The medical trial data and predicted CFD results correlate strongly with the hypothesis that coronary haemodynamics due to stent design are a significant factor in whether or not the stenting procedure will be successful. In light of this evidence, future stent designs should strive to reduce restenosis encouraging haemodynamic effects, primarily regions of low WSS and high WSSG.

This work has demonstrated the ability of applied computer science to provide the biomedical community with insights into complex haemodynamics that can be used to assist in the development of optimal stent designs for the future.

Acknowledgements

This study has been funded by the Dept. of Mechanical Engineering, DIT, and also by the Embark Initiative managed by the IRCSET as part of the National Development Plan, Ireland 2000 - 2006.

References

[1] D. L. Fischman, M. B. Leon, & D. S. Baim, A Randomized Comparison of Coronary Stent Placement and Balloon Angioplasty in Treatment of Coronary Artery Disease, *New England Journal of Medicine, 331*(1), 1994, 496-501.

[2] M. Haude, R. Erbel, H. Issa, & J. Meyer, Quantitative Analysis of Elastic Recoil After Balloon Angioplasty and After Intracoronary Implantation of Balloon-Expandable Palmaz-Schatz Stents, *Journal of the American College of Cardiology, 21*(1), 1993, 26-34.

[3] P. W. Serruys, P. De Jaegere, & F. Kiemeneij, Comparison of Balloon-Expandable-Stent Implantation with Balloon Angioplasty in Patients with Coronary Heart Disease, *New England Journal of Medicine, 331*(1), 1994, 489-495.

[4] J. Garasic, E. R. Elazer, J. C. Squire, P. Seifert, M. Williams, & C. Rogers, Stent and Artery Geometry Determine Intimal Thickening Independent of Arterial Injury, *Circulation, 101*(1), 2000, 812-818.

[5] J. F. LaDisa, L. E. Olson, R. C. Molthen, D. A. Hettrick, P. F. Pratt, M. D. Hardel, J. R. Kersten, D. C. Warltier, & P. S. Pagel, Alterations in Wall Shear Stress Predict Sites of Neointimal Hyperplasia After Stent Implantation in Rabbit Iliac Arteries, *American Journal of Physiology, 288*(1), 2005, H2465-H2475.

[6] C. Unterberg, D. Sandrock, & N. Klaus, Reduced Acute Thrombus Formation Results in Decreased Neointimal Proliferation After Coronary Angioplasty, *Journal of the American College of Cardiology, 26*(7), 1995, 1747-1754.

[7] T. Seo, L. Schachter, & A. Barakat, Computational Study of Fluid Mechanical Disturbance Induced by Endovascular Stents, *Annals of Biomedical Engineering, 33*(4), 2005, 444-456.

[8] J. J. Wentzel, D. Whelan, & W. Van Der Giessen, Coronary Stent Implantation Changes 3-D Vessel Geometry and 3-D Shear Stress Distribution, *Journal of Biomechanics*, *33*(1), 2000, 1287-1295.

[9] C. Brown, Morphological, Biochemical, and Functional Changes in Human Platelets Subjected to Shear Stress, *Journal of Laboratory and Clinical Medicine, 86*(1), 1975, 462-471.

[10] A. M. Malek, S. L. Alper, & S. Izumo, Hemodynamic Shear Stress and its Role in Atherosclerosis, *Journal of the American Medical Association, 282*(21), 1999, 2035-2042.

[11] N. DePaola, M. Gimbrone, P. F. Davies, & C. F. Dewey, Vascular Endothelium Responds to Fluid Shear Stress Gradients, *Arteriosclerosis and Thrombosis, 12*(1), 1992, 1254-1257.

[12] C. Rogers, & E. R. Edelman, Endovascular Stent Design Dictates Experimental Restenosis and Thrombosis, *Circulation, 91*(1), 1995, 2995-3001.

[13] H. Jung, J. W. Choi, & C. G. Park, Asymmetric Flows of Non-Newtonian Fluids in a Symmetric Stenosed Artery, *Korea-Australia Rheology Journal*, *16*(1), 2004, 101-108.

[14] L. Waite, *Biofluid Mechanics in Cardiovascular Systems* (NY: McGraw-Hill, 2006).

[15] A. J. Lansky, G. S. Roubin, C. B. O'Shaughnessy, P. B. Moore, & L. S. Dean, Randomized Comparison of the GR-II Stent and Palmaz-Schatz Stent for Elective Treatment of Coronary Stenoses, *Circulation, 102*(1), 2000, 1364-1368.